Computational Investigation of Oblique Detonation Ramjet-in-Tube Concepts

D. C. Brackett* and D. W. Bogdanoff†
University of Washington, Seattle, Washington

Ramjet-in-tube techniques have been proposed to accelerate masses up to thousands of kilograms to velocities of 0.7–12.0 km/s by chemical means. CFD calculations for three oblique detonation ramjet-in-tube drive modes are presented; the operational velocities for the present results range from 3.5 to 10.0 km/s. The first drive mode achieves ignition on the reflection of the nose cone bow shock. The second drive mode relies on a sudden, steep, but small increase in projectile radius to initiate a detonation wave, following a deliberately gentle, gradual compression process. The third drive mode is similar to the second mode except that the projectile is thermally protected by flying it through a core of pure hydrogen gas surrounded by a detonable mixture. At optimum operating conditions, the thrust pressure ratios (defined as the effective thrust pressure divided by the maximum cycle pressure) for the three modes range from 0.12 to 0.30, and the efficiencies (defined as the thrust times the velocity divided by the rate of chemical energy release) range from 0.09 to 0.26. Tables of thrust pressure ratios and efficiency data and representative plots of the pressure fields around the projectiles are presented.

I. Introduction

STUDIES carried out at the University of Washington since mid-1983 have led to a promising new technique called the "ram accelerator," by which relatively large masses (up to thousands of kilograms) can in principle be efficiently accelerated to velocities up to 12 km/s by utilizing chemical energy in a new manner.[1-5] While the gasdynamic principles of the ram accelerator are similar in many respects to those of the conventional airbreathing ramjet, the device is operated in a different manner. A conventional ramjet consists of an outer cowling and an internal body comprising a forward supersonic diffuser, a combustion section, and a convergent-divergent nozzle. In the ram accelerator concept, the internal body is a projectile fired into a tube and the cowling is now the wall of the tube. This affords the ability to control the pressure, composition, chemical energy density, and speed of sound (and hence Mach number) of the gas entering the ramjet engine. The gaseous propellant, consisting of premixed fuel and oxidizer such as methane and oxygen or hydrogen and oxygen, fills the tube so that no fuel or oxidizer need be carried by the projectile. Since the fuel and oxidizer are premixed, the difficulties in obtaining rapid and complete mixing encountered in conventional subsonic combustion and supersonic combustion ramjets are circumvented.

A number of modes of ram accelerator operation, which in principle span the velocity range of 0.7–12 km/s, have been developed and studied. These include two subsonic combustion modes (one of which involves thermally choked combustion), a normal overdriven detonation mode, and several oblique detonation modes. The oblique detonation type 1 mode achieves ignition on the reflection of the projectile nose cone shock (Fig. 1). The oblique detonation type 2 mode relies on a sudden, steep, but small increase in projectile radius to initiate a detonation wave (Fig. 2). In this case, the compression process upstream of the steep radius increase is made gradual enough not to initiate combustion. The remainder of this paper deals with computational studies of the oblique detonation modes. Details of the other modes are presented elsewhere.[1,3,5] In Sec. II, the computational method used in the investigation of the oblique detonation modes is described briefly. Section III presents a detailed discussion of the computational results.

II. Computational Method

The computational method is described briefly herein. Additional details are given in Ref. 6. The code is two-dimensional and axisymmetric and can be divided in the radial direction into multiple zones containing different media. The gridding can slide in the radial direction to preserve the integrity of the media of the zones. The governing equations are the two-dimensional Euler equations, written in conservation form.

A gas equation of state is used that is perfect volumetrically and takes $e = \int C_v \, dT$ from the JANNAF tables,[7] where e is

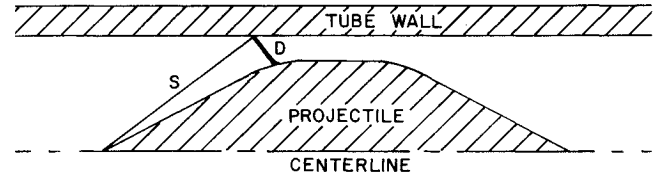

Fig. 1 Oblique detonation type 1 mode. *S* denotes nose cone shock wave and *D*, oblique detonation wave.

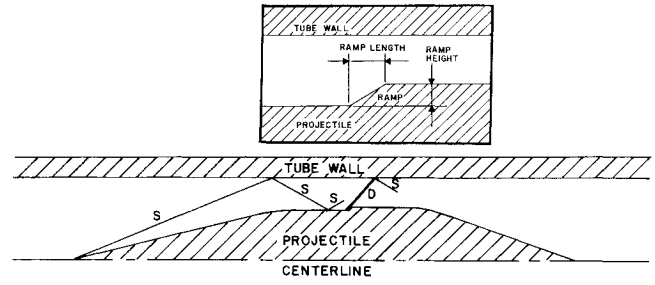

Fig. 2 Oblique detonation type 2 mode. *S* denotes shock waves and *D*, oblique detonation wave. Inset: Magnified view of ramp with length and height indicated. The ramp size is exaggerated compared to the projectile to tube wall spacing.

Received Jan. 25, 1988; revision received June 30, 1988.

*Graduate Student, Aerospace and Energetics Research Program. Student Member AIAA.

†Research Engineer, Aerospace and Energetics Research Program. Member AIAA.

internal energy, C_v is specific heat at constant volume, and T is temperature. Combustion is modeled with a single global Arrhenius expression for reactants → products. The products include all major mass fraction species with fixed mass fractions determined from separate equilibrium combustion calculations.

All results presented in the following section are obtained from converged steady-state solutions. These solutions converge faster than the time required for an appreciable increase in projectile velocity, and hence, the steady-state solutions should be close approximations to flows over a real accelerating projectile.

Rough estimates of viscous and high-temperature effects were made to check the validity of neglecting them in the flowfield calculations. These estimates were based on a carbon projectile traveling at 9.0 km/s in a mixture of $8H_2 + O_2$ at 1.0×10^8 dyne/cm^2 and 300 K, which is typical of the following cases presented. The Reynolds number based on projectile length is on the order of 1.0×10^9; therefore, the boundary layer is assumed to be turbulent and has an estimated momentum thickness at the end of the projectile of about 1% of the maximum projectile radius. Hence, the external flowfield is little influenced by the boundary layer. As for radiational effects, the estimated black-body heat flux at the projectile surface is only about 7% of the convective heat flux. Since this represents the maximum possible radiative heat flux, neglecting radiation is reasonable for these calculations.

Rough estimates of skin friction and ablation were made using the skin-friction calculation techniques of van Driest[8] modified using the data and correlations of Jeromin[9] and Knuth and Dershin[10] to allow for ablation effects. Friction was found to reduce thrust and efficiency by 20–50%, depending on velocity and whether or not ablation occurred. Also, the estimated retreat of the projectile surface was only about 1% of the maximum projectile radius for acceleration up to 6 km/s, and then became large very rapidly. One method for reducing ablation is the use of the stratified charge mode discussed in the next section.

III. Discussion of Results

A. Type 1 Oblique Detonation Mode

In the type 1 detonation mode, the projectile is injected into a tube section at a speed higher than the detonation speed of the surrounding gas mixture. Flow parameters are chosen so that the first or second reflection of the conical nose shock initiates combustion (Fig. 1). A detonation wave develops at the reflected shock front, where combustion occurs in a thin layer. The heated gas expands through the nozzle formed by the projectile rear and tube wall, producing thrust.

We investigated the following gas mixtures at an initial temperature of 300 K and pressure of 1.0×10^8 dyne/cm^2:

1) $8H_2 + O_2$
2) $2H_2 + O_2 + 3.48CO_2$
3) $2H_2 + O_2 + 2N_2$
4) $2H_2 + O_2 + 6N_2$
5) $2H_2 + O_2$

The projectile shape studied consisted of a conical nose section, a cylindrical center section, and a conical tail section (Fig. 1). The transitions from nose to center section and from center section to tail were faired with parabolic curves. Performance surveys were conducted to optimize the projectile-to-tube wall radius ratio, using a fixed tube radius of 1.5 cm and nose and tail half-angles of 14 deg. The tube radius was somewhat arbitrarily chosen but is reasonable for a laboratory device. In the surveys, the projectile length was held constant at 14.7 cm; as the maximum projectile radius was varied, the length of the center section also varied, since the nose and tail angles were kept constant. These surveys were done at a projectile velocity of 7.0 km/s in mixture 1, based on previous one-dimensional calculations of oblique detonation mode performance.[1] The optimal projectile radius was determined to be 1.29 cm. This optimum was selected to maximize the thrust pressure ratio, which is defined as the thrust divided by the projectile cross-sectional area divided by the maximum pressure occurring anywhere on the projectile or tube wall. This ratio is an important performance parameter as it provides a measure of the device's launch capability vs the maximum pressure that the projectile and barrel must survive. Another important parameter is the ballistic efficiency, defined as thrust times projectile velocity divided by the rate of chemical energy release in the combusting flow.

The velocity operating envelope was then determined by varying the velocity of the 1.29-cm-radius projectile. Each case required about 30 h CPU time on a DEC MicroVAX II computer. The projectile velocity was reduced until no combustion occurred due to insufficient heating of the mixture through the shock waves. The lower operating limit for mixture 1 was 6.25 km/s. A case at 5.5 km/s resulted in no combustion and negative thrust. At 6.25 km/s, combustion stabilized at the second reflection of the initial conical shock wave, degrading performance. The upper velocity limit for mixture 1 was 9.0 km/s. At 10.0 km/s, the leading shock wave strength was sufficient to initiate combustion prematurely, subjecting the projectile nose to high pressure and resulting in negative thrust.

Similar surveys were done for the other four gas mixtures. Figure 3 shows curves of thrust pressure ratio vs projectile velocity for all five gas mixtures. Figure 4 shows the corresponding efficiency curves. For mixture 1, it is evident that the optimal operating velocity is near 7.0 km/s, having a thrust pressure ratio of 0.12 and an efficiency of 0.26. This thrust pressure ratio corresponds to a thrust of 3.13×10^9 dynes. Three important results can be obtained from Figs. 3 and 4. First, the velocity range of operation of a projectile can be extended by changing the molecular weight of the diluent gas. The operating range of the projectile can be increased from 6.25–9.0 to 3.5–9.0 km/s by using nitrogen as a diluent at the lower velocities. Second, if there is too much diluent (e.g., mixture 4), the mixture becomes very weak, and low thrust

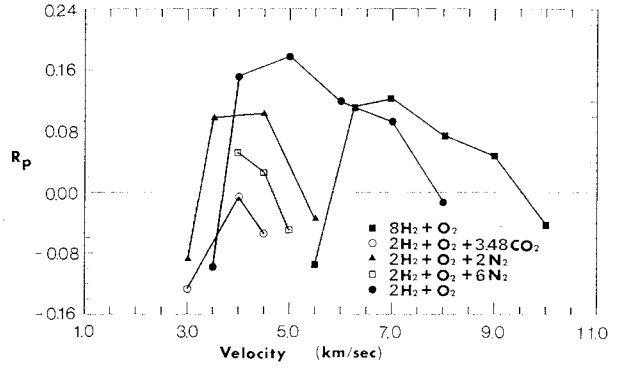

Fig. 3 Oblique detonation type 1 thrust pressure ratio vs projectile velocity.

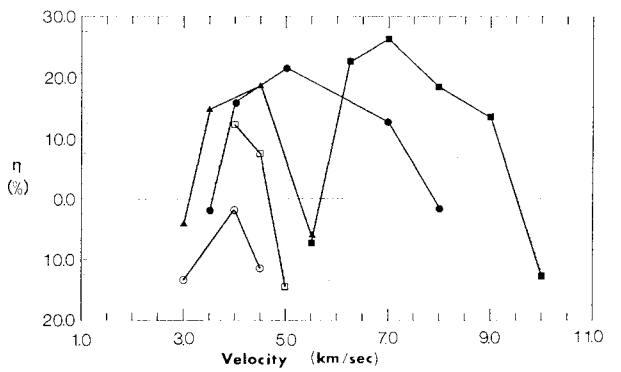

Fig. 4 Oblique detonation type 1 ballistic efficiency vs projectile velocity. Gas mixtures are the same as in Fig. 3.

pressure ratios and efficiencies are obtained. The minimum amount of diluent should therefore be used, consistent with the desired velocity range. Third, lower specific heat ratio diluents (e.g., mixture 2) produce lower or negative thrust pressure ratios and efficiencies. The present CFD results bear out earlier one-dimensional computational studies in this respect.[1]

We produced graphical code results using a standard contour plotting package. Figure 5 illustrates the pressure contours around the projectile moving at 7.0 km/s in mixture 1. Note that only the outer third of the flowfield is shown for clarity. The nose of the projectile is, therefore, well to the left of the $x = 0$ point. Going from left to right in the flowfield, we see the nose cone shock, the reflected oblique detonation wave impinging on the projectile at the forward projectile shoulder, a series of reflections of shocks and expansion waves of decreasing strength over the center section of the projectile, and finally, the expansion wave system over the tail of the projectile.

B. Type 2 Oblique Detonation Mode

In the type 2 oblique detonation mode, combustion is initiated in a different manner. Whereas careful flow parameter "tuning" is necessary for successful ignition in the type 1 mode, the onset of combustion is "forced" in the type 2 mode by the insertion of a steeply sloped ramp in the projectile profile at the location where ignition is desired (Fig. 2). The resulting sharp compression of the combustible gas produces a detonation wave that is stationary with respect to the projectile. The ramp may be split into discrete bumps spaced azimuthally around the projectile body to reduce the drag penalty on the forward slopes of the bumps. Since our code is axisymmetric, the ramp has to be axisymmetric, extending completely around the projectile. The drag on the forward-facing surfaces of the ramp will degrade the performance more than if discrete bumps were used. Therefore, we calculated two sets of thrust pressure ratio and cycle efficiency values for each case studied. One set includes the effect of the additional drag on the initiation ramp, while the other ignores it. Thus, the values for the corresponding discrete bump configuration are bracketed. Also, for the type 2 oblique detonation mode calculations, thrust pressure ratios were calculated based on the maximum pressure exerted on the projectile, excluding tube wall pressures. Maintaining projectile integrity under sustained high-pressure loading is necessary, of course. Although the tube wall may experience higher pressures, even in excess of its yield stress, the duration of the loading can be made short enough that the material does not deform sufficiently to yield. Using the barrel in this mode permits higher operating pressures, proportionately reducing the barrel length required to achieve a given velocity.

As in the type 1 oblique detonation studies, we ran type 2 projectile geometry optimization tests at 7.0 km/s in mixture 1. About 75 h CPU time on a DEC MicroVAX II computer were required to complete each of these cases. Because nose shock strength was no longer critical in the ignition process, a more slender nose cone half-angle of 7 deg was chosen to extend the high-speed predetonation velocity limit beyond that of the type 1 mode. A rear cone angle of 10 deg was chosen to limit the flow expansion rate. If the rear cone angle is too large, the expansion wave system on the rear of the projectile can cause the pressures on the rear cone to drop so low that the thrust is severely degraded. Also, if the angles are larger still, code failure can occur when densities and internal energies attempt to go to zero in the expansion wave system.

We found that with a ramp length of 0.135 cm, a ramp height of 0.04 cm (see Fig. 2) was the minimum necessary to initiate combustion reliably at this velocity. The maximum radius for the optimized projectile (with respect to thrust pressure ratio and efficiency) was 1.0 cm for the type 2 mode vs 1.29 cm for the type 1 mode (for a 1.5-cm-radius tube). The smaller value was chosen because higher thrust pressure ratios were obtained while maintaining satisfactory cycle efficiency. Performance parameters proved to be very sensitive to projectile length and ramp placement. If the ramp is considerably upstream of the point where the reflection of the nose cone shock intersects the projectile surface, the gas impinging on the ramp is relatively expanded and cool and ignition is very difficult. On the other hand, by placing the ramp somewhat downstream of the point where the reflection of the nose shock intersects the projectile surface, the gas impinging on the ramp is relatively compressed and hot, making ignition much easier.

In the region downstream of the detonation wave, the location of the reflected wave pattern relative to the projectile surface proved to be very important. Thrust is only developed when high pressures occur on the tail of the projectile. Highest thrusts are obtained when a reflection of the oblique detonation wave impinges on the projectile in the neighborhood, but somewhat downstream of, the rear shoulder of the projectile. Large differential thrust elements are then produced on the upstream part of the tail, which, of course, carries the majority of the possible thrust-producing area. If the wave system is disposed with respect to the projectile so that this critical part of the projectile tail is in a relatively low-pressure expansion region, the projectile performance is much poorer. The exact

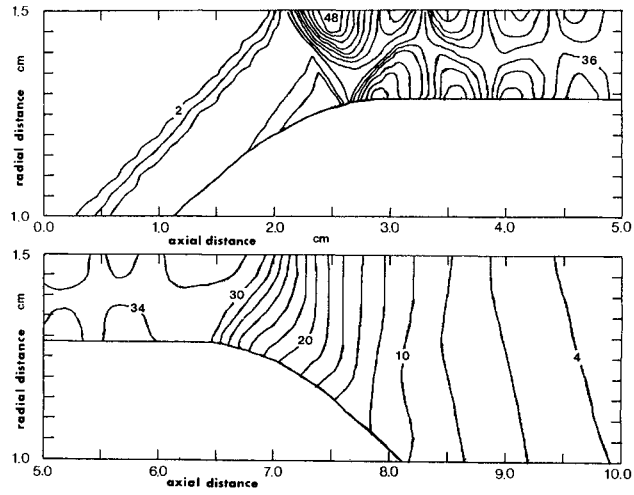

Fig. 5 Pressure contours surrounding oblique detonation type 1 projectile moving at 7.0 km/s in mixture 1 ($8H_2 + O_2$). The pressure values shown are scaled by 1.0×10^{-8} dyne/cm^2. The vertical scale is exaggerated 3.51 times.

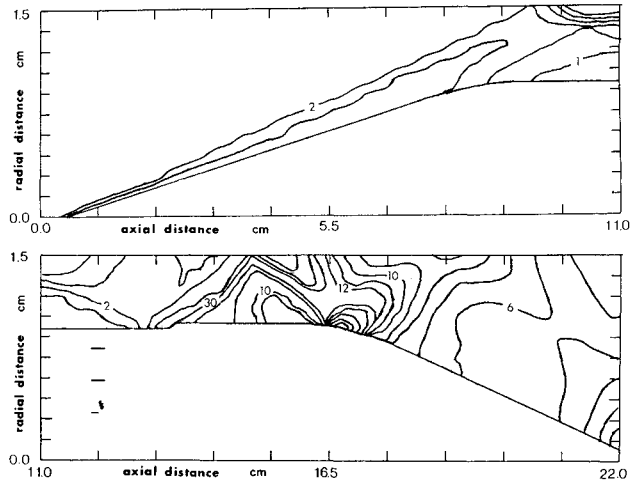

Fig. 6 Pressure contours surrounding oblique detonation type 2 projectile with a 0.04-cm-high ramp moving at 8.0 km/s in mixture 1 ($8H_2 + O_2$). The pressure values shown are scaled by 1.0×10^{-8} dyne/cm^2. The vertical scale is exaggerated 2.57 times.

disposition of the wave system varies, of course, with projectile velocity, but, as will be shown, a properly designed projectile does have a substantial range of operating velocities in a given gas mixture.

Figure 6 illustrates the pressure wave pattern surrounding a 22.5-cm projectile traveling at 8.0 km/s in mixture 1. In Fig. 6, we can see the nose cone shock, followed by the expansion wave emanating from the front shoulder of the projectile. The nose cone shock reflects from the tube wall and impinges on the projectile somewhat upstream of the ramp. The ramp initiates the oblique detonation wave, which then reflects as a shock from the tube wall and impinges on the projectile near the rear shoulder. The expansion flow over the projectile tail is complicated by two further reflections of the oblique detonation wave shocks and the expansion wave system emanating from the rear shoulder. There is some recompression near the rear tip of the projectile due to flow turning.

Projectile lengths of 20.0, 22.0, and 22.5 cm were studied. The only difference between these three projectiles was the length of the cylindrical section downstream of the ramp. Type 2 oblique detonation thrust pressure ratio and efficiency results are shown in Figs. 7 and 8, respectively. At 7.0 km/s in mixture 1, the 20.0-cm projectile exhibited the highest thrust pressure ratio of 0.301, corresponding to a thrust of 2.28×10^9 dynes. The 22.5-cm projectile achieved a maximum thrust pressure ratio of 0.279 at 9.0 km/s in mixture 1, corresponding to a thrust of 2.15×10^9 dynes. These values do not include the drag produced by the ramp, and the thrust pressure ratios are based on the maximum pressure experienced by the projectile itself. Table 1 compares these results with those from the type 1 oblique detonation study using mixture 1. Thrust pressure ratio R_p and cycle efficiency η values are also given, calculated using 25% of the ramp drag to simulate a projectile with discrete bumps occupying 25% of the 2π azimuthal ramp angle.

Using the values from Table 1, including 25% ramp drag, we see that R_p values for the type 2 mode (0.26–0.28) are much greater than those for the type 1 mode (0.05–0.12) for the velocity range studied here. The efficiency of the type 1 mode is greater than that of the type 2 mode at 7 km/s but less at 9 km/s. Our opinion is that, overall, the type 2 mode is superior, R_p being greater for this mode by a factor of $\sim$2.3–5.0, while η is comparable or, at worst, less by a factor of $\sim$1.5.

A velocity survey revealed that the longer projectile operated over a wider velocity range in the same mixture. The highest successful velocity was 7.5 km/s for the 20.0-cm projectile and 9.0 km/s for both the 22.0- and 22.5-cm projectiles. For the type 2 mode, high velocity failure occurs when the detonation and its reflected wave system become stretched out toward the projectile rear to the point that the critical thrust-producing area of the upstream part of the projectile tail is mainly subject to relatively low pressures. The net thrust then becomes negative. The high-velocity failure mechanism for the type 2 mode is thus quite different than that for the type 1 mode, where the high-velocity failure mechanism is predetonation on the initial nose shock. The combustible gas mixture can be varied as necessary along the tube length to control the flight Mach number and retain a near optimal thrust-producing flow pattern.

C. Stratified Charge Mode

At velocities above about 6.0 km/s, ablation problems must be addressed. One proposed method to reduce the stagnation temperatures experienced by the projectile body is to fly it through a pure hydrogen gas core surrounded by a combustible gas mixture. The resulting increase in the speed of sound of the core flow reduces the Mach number and, therefore, lessens the severity of projectile nose heating and mass loss due to ablation. Also, the relatively cool hydrogen would provide an effective thermal shield between the hot combustion products and the projectile surface. This technique would also greatly reduce the frictional drag on the projectile.

The multiple material zone capability of the code can be used to model such a scenario. Case studies of a type 2 oblique detonation projectile flying through such a stratified gas have been made. The gas was stratified as follows. A 1.5-cm-radius tube contained pure hydrogen gas from the center to half-tube radius; the remainder of the tube was filled with a stoichiometric hydrogen-oxygen mixture. The computational model contained six cells in the radial direction in each of the two gas zones. The interzone boundary was assumed impermeable but movable.

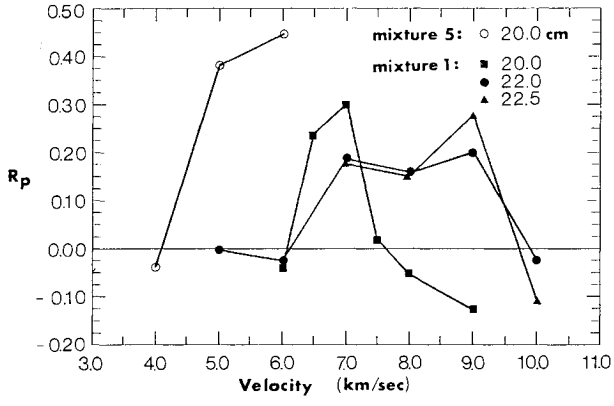

Fig. 7 Oblique detonation type 2 thrust pressure ratios vs projectile velocity for projectile lengths and gas mixtures indicated.

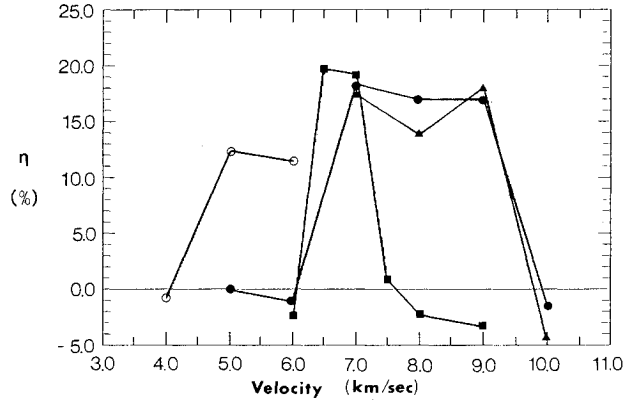

Fig. 8 Oblique detonation cycle efficiency vs projectile velocity for projectile lengths and gas mixtures indicated in Fig. 7.

Table 1 Comparison of type 1 and type 2 oblique detonation modes performances

Mode	Velocity, km/s	Length, cm	Ramp drag ignored		25% ramp drag	
			R_p	η	R_p	η
Type 2	7.0	20.0	0.301	0.192	0.281	0.180
Type 2	9.0	22.5	0.279	0.181	0.259	0.168
Type 1	7.0	14.7	0.123	0.264	—	—
Type 1	9.0	14.7	0.048	0.134	—	—

A projectile having a 7-deg nose cone half-angle and a 1.0-cm radius upstream of the ramp moving at 10.0 km/s through a 1.0×10^8-dyne/cm^2 stratified mixture was taken as a benchmark case. As for the type 2 oblique detonation mode, the initiation ramp was located somewhat downstream of the location where the reflection of the nose cone shock intersects the projectile surface. For a ramp length of 0.135 cm, as was used for the type 2 oblique detonation case, a survey was conducted to determine the minimum ramp height necessary to initiate combustion in the outer gas zone. The maximum height investigated was 0.050 cm. A ramp height of 0.035 cm was found to be the smallest necessary to promptly initiate combustion throughout the outer combustible gas zone at 10.0 km/s, corresponding to an angle of 14.5 deg. A 0.030-cm ramp height also propagated a shock wave of sufficient strength to ignite the outer mixture. However, the point of complete combustion was downstream of the ramp location by about 3.0 cm, requiring a longer projectile for only a moderate decrease in ramp drag. (The ramp drag for ramp heights of 0.030 and 0.035 cm were 0.320 and 0.444 times that for a 0.050-cm ramp height, respectively.) Therefore, the 0.035-cm ramp height was chosen for further study. The ramp drag for the 0.035-cm ramp height case was 0.235 times the projectile thrust obtained ignoring ramp drag.

Since ignition does not occur on the ramp itself in the stratified charge mode, but rather in the outer gas zone, the shock wave produced by the ramp (or bumps in the three-dimensional case) must retain sufficient strength through the core gas zone. Therefore, discrete bumps would likely have to cover more projectile circumference than in the single-gas zone oblique detonation type 2 mode. A figure of 50% circumferential coverage was arbitrarily chosen for the stratified charge mode performance parameter calculations. A 25% circumferential (azimuthal) coverage had been used for the single-gas oblique detonation type 2 mode calculations. Tail cone half-angles of 10 and 5 deg were investigated. Both produced positive thrust, but the more gradual expansion of the 5-deg case resulted in a higher efficiency and thrust pressure ratio than was achieved by the 10-deg tail, as shown in Table 2. For tail angles of 10 and 5 deg, the projectile lengths were 28.5 and 33.6 cm, respectively. It is possible that the previously discussed oblique detonation modes would also benefit from a more gradual expansion, but the high velocity limitations of the type 1 mode and the severity of the projectile heating of the type 2 mode would not be affected.

Figure 9 illustrates the pressure field produced by a projectile with a 0.035-cm ramp height and a 5-deg tail half-angle operating at 10.0 km/s in the stratified charge mode. In Fig. 9, one can see the nose cone shock, followed by the expansion wave emanating from the front shoulder of the projectile. The nose cone shock reflects from the tube wall and intersects the projectile surface somewhat upstream of the initiation ramp. The initiation ramp propagates a shock wave out toward the detonable gas mixture, which detonates, propagating detonation/shock waves both outward toward the tube wall and inward toward the projectile. The reflection of the detonation wave from the tube wall then impinges on the projectile in the neighborhood of the rear shoulder, essentially canceling the expansion wave system that normally would emanate from this shoulder. Thus, the pressure is kept reasonably high on the critical thrust-producing area of the forward part of the projectile tail, and good performance is obtained. Note that the hydrogen core, indicated by the dotted line, is very much volumetrically compressed following the initiation of the detonation wave.

Since the computational model is inviscid and has a zone boundary at the gas interface, turbulent mixing at the interface shear layer is not modeled. A large amount of turbulent mixing could cause the protection of the projectile by the hydrogen core to be compromised. Rough estimates of the shear-layer spreading rate have been made; these suggest that thermal protection of the projectile using a hydrogen core, as

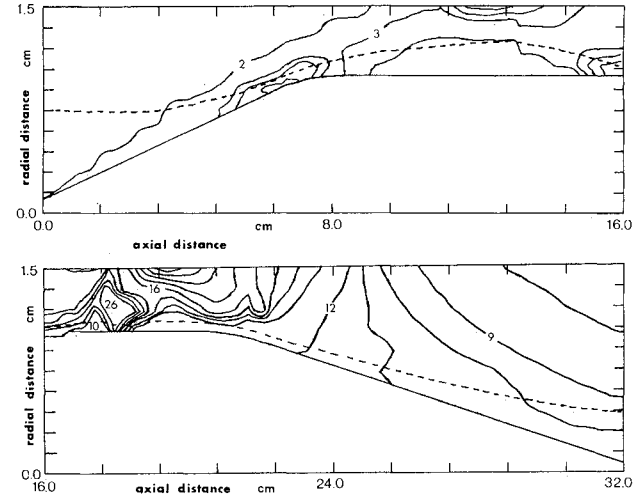

Fig. 9 Pressure contours surrounding a projectile with a 0.035-cm-high ramp height moving at 10.0 km/s in a stratified charge with an H_2 core surrounded by a $2H_2 + O_2$ mixture. The pressure values shown are scaled by 1.0×10^{-8} dyne/cm^2. The vertical scale is exaggerated 3.93 times. The gas interface is shown dashed.

Table 2 Performance of stratified charge mode

Ramp height, cm	Tail half-angle, deg	Ramp drag ignored		50% ramp drag	
		R_p	η	R_p	η
0.050	10	0.134	0.076	0.088	0.050
0.050	5	0.191	0.108	0.145	0.082
0.035	5	0.283	0.100	0.250	0.088

Table 3 Comparison of type 1 and type 2 oblique detonation and stratified charge modes

Mode	Velocity, km/s	Ramp height, cm	Ramp drag ignored		Partial ramp drag	
			R_p	η	R_p	η
Type 1 oblique detonation	9.0	(No ramp)	0.048	0.134	—	—
Type 2 oblique detonation	9.0	0.040	0.279	0.181	(25% ramp drag) 0.259	0.168
Stratified charge	9.0	0.040	0.269	0.104	(50% ramp drag) 0.214	0.082
Stratified charge	10.0	0.035	0.283	0.100	0.250	0.088

proposed in the stratified charge mode, may well be feasible, even allowing for shear-layer spreading.

Substantial reduction of stagnation temperature at the projectile surface is afforded by the stratified charge mode. At 10.0 km/s, the peak stagnation temperature at the surface of a projectile having a 0.035-cm ramp is 3310 K, compared to ~8000 K estimated for the same projectile at the same velocity in a uniform $8H_2 + O_2$ mixture. (The latter temperature was estimated from code output parameters and assumes an average specific heat value estimated from the JANNAF tables.[7]) The problem of projectile ablation is, therefore, greatly reduced by employing the stratified charge configuration.

Table 3 compares the highest operating velocity cases for the type 1 and type 2 oblique detonation modes and the stratified charge mode. Only the stratified charge mode operated successfully at 10.0 km/s, producing a thrust of 2.04×10^9 dynes, including ramp drag. For direct comparison with the other two modes, a stratified charge test case was run at 9.0 km/s with a ramp height of 0.04 cm and a 5-deg tail. The R_p for the stratified charge mode at 9.0 km/s was 17% less than the R_p for the type 2 oblique detonation mode at 9.0 km/s, but more than four times the R_p for the type 1 oblique detonation mode at 9.0 km/s. There is a penalty for the use of the stratified charge with respect to efficiency, however. Referring to Table 3, the stratified charge case has an efficiency of 0.082 at 9.0 km/s vs efficiencies of 0.134 and 0.168 at 9.0 km/s for the type 1 and type 2 oblique detonation modes, respectively.

At 10.0 km/s with a ramp height of 0.035 cm, the stratified charge mode produced higher values of R_p and efficiency, 0.250 and 0.088, respectively. Referring to Table 3, this value of R_p compares favorably with the type 2 oblique detonation mode at 9.0 km/s and is more than five times the R_p for the type 1 oblique detonation mode at 9.0 km/s. Again, there is a penalty for the use of the stratified charge with respect to efficiency. The stratified charge case has an efficiency of 0.088 at 10.0 km/s vs efficiencies of 0.134 and 0.168 at 9.0 km/s for the type 1 and type 2 oblique detonation modes, respectively. It may be possible to raise the efficiency of the stratified charge mode somewhat by increasing the maximum radius of the projectile. This increase in η would probably be accompanied by a decrease in R_p.

IV. Conclusions

Ramjet-in-tube techniques can, in principle, be used to accelerate masses up to thousands of kilograms to velocities up to 10.0 km/s by chemical means. CFD calculations of three oblique detonation ramjet-in-tube drive modes have been presented; the widest operating velocity range demonstrated here is 3.5–10.0 km/s. At optimum operating conditions, the thrust pressure ratios (defined as the effective thrust pressure divided by maximum cycle pressure) for the three modes range from 0.12 to 0.30, and the efficiencies (defined as the rate of change of kinetic energy divided by the rate of chemical energy release) range from 0.09 to 0.26.

Experimental verification of these computational studies will be conducted at the University of Washington at velocities in the 2–3 km/s range. Higher velocity verification will be pursued in other facilities at later dates.

Acknowledgments

The work was supported in part by USAF Contract F08635-84-K0143 and in part by DOE Contract DE-FG06-85ER13382. The authors would like to acknowledge a number of very informative conversations with R. W. MacCormack, D. S. Eberhardt, A. Hertzberg, and A. P. Bruckner during the course of this work.

References

[1]Bruckner, A. P., Bogdanoff, D. W., Knowlen, C., and Hertzberg, A., "Investigations of Gasdynamic Phenomena Associated with the Ram Accelerator Concept," AIAA Paper 87-1327, June 1987.

[2]Bogdanoff, D. W. and Brackett, D. C., "A Computational Fluid Dynamics Code for the Investigation of Ramjet-in-Tube Concepts," AIAA Paper 87-1978, June–July 1987.

[3]Knowlen, C., Bogdanoff, D. W., Bruckner, A. P., and Hertzberg, A., "Performance Capabilities of the Ram Accelerator," AIAA Paper 87-2152, June–July 1987.

[4]Hertzberg, A., Bruckner, A. P., Bogdanoff, D. W., and Knowlen, C., "The Ram Accelerator and Its Applications: A New Chemical Approach for Reaching Ultrahigh Velocities," Grönig, H. (ed.), *Proceedings of the 16th International Symposium on Shock Tubes and Waves*, Aachen, UCH Verlagsgesellshaft mbH, Weinheim, FRG, 1988, pp. 117–128.

[5]Hertzberg, A., Bruckner, A. P., and Bogdanoff, D. W., "The Ram Accelerator: A New Method for Accelerating Projectiles to Ultrahigh Velocities," *AIAA Journal*, Vol. 26, Feb. 1988, pp. 195–203.

[6]Bogdanoff, D. W. and Brackett, D. C., "A Godunov CFD Method for Extreme Flow Velocities and Any Equation of State," *AIAA Journal* (to be published).

[7]Stull, D. R. and Prophet, M., project directors, *JANNAF Thermochemical Tables*, U.S. Government Printing Office, Washington, DC, NSRDS-NBS 37, June 1971, p. 4.

[8]van Driest, E. R., "Turbulent Boundary Layer in Compressible Fluids," *Journal of the Aeronautic Sciences*, Vol. 18, March 1951, pp. 145–160, 216.

[9]Jeromin, L. O. F., "The Status of Research in Turbulent Boundary Layers with Fluid Injection," *Progress in Aeronautical Sciences*, Vol. 10, 1970, pp. 65–190.

[10]Knuth, E. L. and Dershin, H., "Use of Reference States in High-Speed Turbulent Flows with Mass Transfers," *International Journal of Heat and Mass Transfer*, Vol. 6, 1963, pp. 999–1018.